Hindawi
Scientific Programming
Volume 2021, Article ID 8382482, 5 pages
https://doi.org/10.1155/2021/8382482

*Research Article*

# Temperature Measurement and Control Application in a Laser Plastic Surgery Real Temperature Detection System

**Hong Wei**,[1] **Fang Jiang**,[1] **Fang Shao**,[1] **Denghui Zhang**,[1] **Fang Gu**,[2] **Ying Yang**,[1] **Qiuxia Chen**,[1] **and Zheng Ai**[1]

[1]*Tianyou Hospital Affiliated to Wuhan University of Science & Technology, Wuhan 430064, China*
[2]*Zhejiang Provincial People's Hospital, Zhejiang 310014, China*

Correspondence should be addressed to Qiuxia Chen; chenqiuxiajgcgk@126.com and Zheng Ai; 0430067@alu.fudan.edu.cn

Received 19 June 2021; Accepted 9 September 2021; Published 28 September 2021

Academic Editor: Arunkumar N



The purpose of this study was to grasp the development process of thermal image temperature measurement technology. It provides directional support for the optimization development of the thermal imagery and laser plastic surgery and laser treatment. This paper uses the infrared thermal image temperature measurement principle and performs infrared thermal image precise temperature measurement technology and its application research. The results showed that there was a correlation between 595 nm pulse dye laser, age, laser energy density, and skin temperature ($P < 0.05$). There is a significant difference in the average ($P < 0.05$). The infrared thermal imagery temperature monitoring system is a simple and relatively accurate temperature detection system that can be widely used in temperature measurement and control of laser plastic surgery.

## 1. Introduction

The infrared thermal imaging technique (IRT) is a noncontact sensing technique, since the object of all surface temperatures exceeds absolute zero, the infrared thermal image can receive these specific electromagnetic wave signals by a photothermal sensor, and then, this signal is converted to an image and graphic of human visual resolution and the temperature value is further calculated, that is, a thermal image map. Based on the region of the vessel distribution density, the blood flow rate is fast, the body surface temperature is also high, and the thermal image generated by the infrared radiation analyses the "hotspot" and surrounding tissue to locate the blood vessel. It is widely used in the medical industry, which has been applied to breast cancer, diabetic neuropathy, vascular disease, skin pathology, heart, fever screening, and brain imaging. In the shaped surgical field, there are many research studies on laser plastic surgery, flap wear testing, burn depth assessment, skin malignant tumor diagnosis, etc. This study intended to explore the clinical application of dynamic infrared thermal imaging techniques (Dirt) in laser plastic surgery treatment.

The operation of the infrared thermal imagery is an infrared radiation that is collected at a certain distance, so its temperature measurement accuracy is vulnerable to external radiation. For the infrared thermal imagery, the measurement distance, the measurement distance between the infrared camera and the measured object, and the atmospheric transmittance, the infrared thermal imager body radiation affects the problem, and to reduce, to maximum limit, the effects of various factors on infrared temperature measurement and to improve the temperature measurement accuracy of the infrared thermal imager, domestic and foreign scholars have conducted a lot of experiments and research.

Le, *J* proposed a two-point calibration method to reduce the influence of the nonuniformity of the detector [1]. The relationship between the temperature of the object and the infrared image grayscale value is obtained by the different temperature, calculating the correction gain coefficient and the offset. Yang H proposed an

artificial neural network method to reduce the influence of nonuniformity of detectors on temperature measurement accuracy, adopting first-input desired error values, then reverse the error forward, realize automatic modification weight, and improve correction effectiveness [2]. Zhao H improved the traditional BP artificial neural network method, proposing a normalized BP artificial neural network correction method, that is, before applying a traditional BP correction algorithm, first, one should make it become the nearby value and finally restore the data, overcoming the difficulty of practical application of practical application due to difficulty in the classic BP algorithm [3]. The research on the temperature accuracy of the infrared thermal imager was conducted several years ago, and the results are relatively backward. Zhao and Zheng integrated the reflectance, the surface emissivity, ambient temperature, atmospheric attenuation, atmospheric temperature, etc. and summarized the effect of the abovementioned error [4]. For the effect of the temperature measurement accuracy, Kale et al. analyzed the influence factor of the temperature-sensing temperature accuracy of the infrared thermal imagery, established the theoretical model of various influence factors on the temperature measurement accuracy, and calculated the temperature error of the object to be measured at different temperature curves [5].

Tapetado et al., through theoretical analysis and practical experience, summarized the method of reducing the error that has a certain use of infrared thermal imaging in the wild [6]. Brian et al. calculated the temperature measurement error curve corresponding to the infrared thermal imagery when the surface emissivity of the object was different [7]. As a result, verification, the temperature measurement accuracy of the infrared thermal imagery becomes high as the surface emissivity of the object. Rainey and Kavner discussed the relationship between the detector characteristics response band and the detection temperature. When the performance of the detector is completely consistent, the temperature detection performance corresponding to the detector of different bands is different, and the guidance selection of different detectors is of great significance [8]. Zou et al. discussed the effects of other high-temperature objects or ambient temperature on the temperature accuracy of the infrared thermal imager, and the theoretical calculation formula of the effects of the measured objects was derived [9].

## 2. Materials, Methods, and Results

This study adopted a forward-looking clinical case study and did not have a control group. The main sample is from the laser treatment room and laser beauty center from 2014 to 2015. All patients' personal basic information and diagnostics, treatment sites, and Fitzpatrick (Photomicidity) skin classification were recorded. The infrared thermal imagery was used to record the patients' infrared image. At the same time, the daily image of the patient treatment site was recorded in the postoperative period, and the postoperative reaction was observed.

*2.1. Thermal Imaging.* The infrared thermal imagery shows the thermal imaging diagram in the pseudocolor state in real time and records. The thermal imager monitor area corresponds to the temperature value of the actual area of the monitoring unit in a single pixel point, and the measurement accuracy is 0.1°C. The thermal imagery software SmartView displays the temperature distribution in the form of a fold line. It is observed that the image is visually displayed in a pseudocolor form and the color tone is from low to high. During the video dynamic recording, the pseudocolor is adjusted in real time with the patients' facial part, and there is a cross mark positioning the absolute value in the measurement area, accurate to 0.1°C.

*2.2. 595 nm Pulse Dye Laser Treatment Temperature Curve.* Among the 45 patients with a 595 nm pulsed dye laser treatment, the treatment of some skin real-time temperature variations in the ink instrument monitoring area is shown in Figure 1.

*2.3. Tune Q 755NM Zi Cui Gem Laser Treatment Temperature Curve.* In 20 patients who were subjected to regulation of Q 755 nm Zijiju laser treatment, the treatment of some skin was relatively stable in the treatment of the instrument monitoring area [10].

*2.4. Long-Pulse-Width (755 nm) Zi Cuiju Laser Treatment Temperature Curve.* In 20 patients who were subjected to regression Q 755 nm Zi-jewel laser therapy, the ink instrument monitoring area has been treated in real time, and the real-time temperature variation curve of real-time temperature variations is shown in Figure 2.

*2.5. Long-Pulse-Width (1064 nm) Nd:YAG Laser Treatment Temperature Curve.* The patients with strawberry-shaped infantile hemangioma treated with long pulse width 1064 Nd:YAG laser were followed up. Through instrument monitoring, it was found that the skin temperature in the laser treatment area increased significantly and was relatively stable.

*2.6. 10600 nm Super Pulse $CO_2$ Laser Treatment Temperature Curve.* The patients who received 10600 nm ultra-pulsed CO2 laser for the treatment of mandibular tumors such as pigment and sweat tumors were followed up. The results showed that there was a large temperature difference between the initial stage and the end of treatment, and the temperature in the middle of treatment remained stable.

## 3. Data Analysis

*3.1. 595 nm Pulse Dye Laser Treatment-Related Data Analysis.* This study randomly selected 55 patients with oral and maxillofacial head and neck from the Ninth People's Hospital of Shanghai Jiaotong University School of Medicine, 55 patients from laser beauty centers, 2014 to 2015, and those

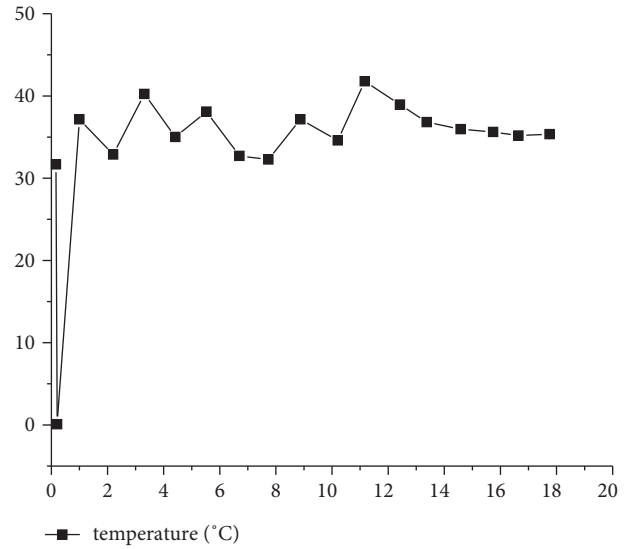


Figure 1: Line diagram of temperature change corresponding to treatment time of 595 nm pulsed dye laser for the treatment of bright red nevus.

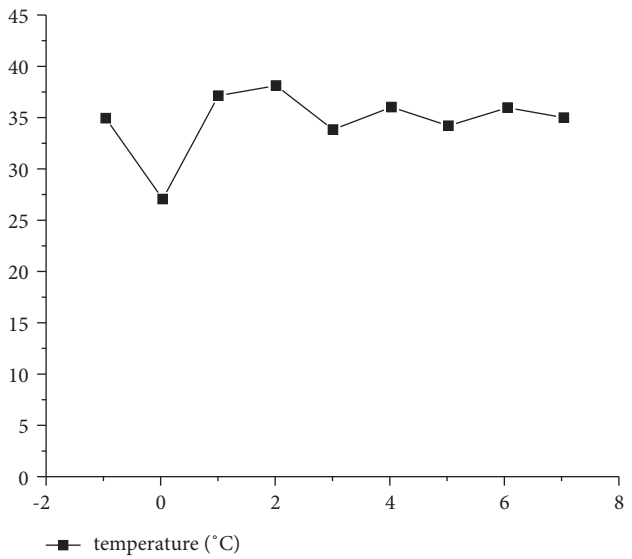


Figure 2: Line diagram of treatment time and temperature change for a long pulse width of 755 nm of emerald laser.

with Fitzpatrick layouts III. Among them, 84 were men and 71 were women.

*3.2. Relationship between Gender and Skin Temperature.* From the independent sample $T$ test analysis of gender and skin temperature, the average skin temperature of the male group and female group has a statistical difference ($P < 0.05$), and the skin temperature of the male group is $44.73 \pm 5.56$, and the skin temperature of the female group is $49.13 \pm 4.15$. Male average skin temperature is lower than that of female. According to 0–10 years old, 11–20 years old, and 21–30 years old age group, we conducted a comparison of the average skin temperature of each age group (Tables 1–3) and found that except 0–10 years old outside of the group, the remaining two groups are the average temperature of male groups than women, and the difference has a statistical significance ($P < 0.05$) [11].

Table 1: 595NM pulse dye laser treatment skin temperature of the 0–10 years age group of male and female by the independent-sample $T$ test.

| Gender | Male | Female |
|---|---|---|
| Number | 32 | 27 |
| Temperature | $43.77 \pm 4.15$ | $44.21 \pm 3.67$ |
| $P$ values | 0.3472 | |

Table 2: 595NM pulse dye laser treatment skin temperature of the 11–20 years age group of male and female.

| Gender | Male | Female |
|---|---|---|
| Number | 31 | 22 |
| Temperature | $44.25 \pm 3.64$ | $47.51 \pm 5.32$ |
| $P$ values | <0.05 | |

Table 3: 595NM pulse dye laser treatment skin temperature of the 21–30 years age group of male and female.

| Gender | Male | Female |
|---|---|---|
| Number | 21 | 22 |
| Temperature | $46.52 \pm 5.11$ | $49.82 \pm 4.66$ |
| $P$ values | <0.05 | |

*3.3. Relationship between Age and Skin Temperature.* From the correlation analysis of age and skin temperature, it is known that the average value is 11.26, the temperature average is 47.68, and the correlation between age and skin temperature is statistically significant ($P < 0.05$).

*3.4. Relationship between Laser Energy Density and Skin Temperature.* From the correlation analysis of laser energy density and skin temperature, it was found that the laser energy density is 7.85, the skin temperature is 47.68, and the correlation between laser energy density and skin temperature has a statistical significance ($P < 0.05$).

*3.5. Multifactor Analysis of Skin Temperature.* The multifactor analysis results (Table 4) of the skin temperature (Table 4) show that there is a correlation between the energy density and the skin temperature ($P < 0.05$).

*3.6. Analysis of Related Data of q 755 nm Zi Cui Gem.* This study randomly selected 55 patients with oral and maxillofacial head and neck from the Ninth People's Hospital of Shanghai Jiaotong University School of Medicine, 55 patients from laser beauty centers, 2014 to 2015, and those with Fitzpatrick layouts III. Among them, 35 were men and 40 were women.

Table 4: Multifactor analysis of skin temperature in the treatment group of 595 nm pulse dye laser.

| | Gender | Age | Energy density |
|---|---|---|---|
| Coefficient | 3.58 | −0.2 | 2.47 |
| 95% confidence interval | [1.70, 5.46] | [−0.46, 0.06] | [−4.22, 9.16] |
| $P$ values | <0.05 | 0.128 | <0.05 |

*3.7. Gender and Skin Temperature Relationship.* According to the independent-sample $T$ test analysis of gender and skin temperature, the skin temperature of the male group is 47.33 and the skin temperature of female group is 49.58. The average skin temperature of the male group and female group has statistical differences ($P < 0.05$), and the female group's average skin temperature is higher than that of the male group [12].

*3.8. Relationship between Age and Skin Temperature.* From the correlation analysis of age and skin temperature, it is known that the average value is 26.73, the temperature average is 48.96, and the correlation between age and skin temperature is not statistically significant ($P > 0.05$).

*3.9. Relationship between Laser Energy Density and Skin Temperature.* From the correlation analysis of laser energy density and skin temperature, it was found that the laser energy density is 7.93, the skin temperature is 48.96, and the correlation between laser energy density and skin temperature is not statistically significant ($P > 0.05$).

## 4. Observation on Skin Reactions after Laser Surgery

*4.1. Follow-Up Observation after Laser Treatment of YAG Laser.* During the treatment of infant hem and juvenile Begonia (strawberry) herpes with bitter gallium aluminum garnet (Nd:YAG) laser with a pulse width of 1064 nm, it was found that blisters were obviously formed in the local area of the treatment, there were congestion bands around, and a small amount of exudate was formed. On the seventh day, the contents of the blister were absorbed. The blister broke and fell off, forming a local wound. After treatment, some small blisters scab, most of them fall, and the redness and swelling subside.

*4.2. 595 nm Pulsed Dye Laser Treatment and Follow-Up Observation after 10600 nm $CO_2$ Laser Treatment.* A 10-year-old patient with right facial (mainly) apical erythema was treated with 595 nm pulsed dye laser, and there was a response corresponding to laser treatment (right oval area). After the treatment of hypertrophic scar with combined dot matrix CO2 laser, the surrounding scar color gradually becomes lighter, and erythema is formed in the surrounding area. Hypertequiode edema affects the scope of the mild activity; the right side face is obviously swollen and asymmetrical with the left side, and there is no obvious blister. On the third day, from the edge region of the lower and upper lip and other lesions, the entire purpura is gradually reduced, and the edema of the tissue loose is obviously resolved; most of the swells have resolved. On the fifth day, the entire purpura continued to decrease, and the loose tissue edema and the face swelling were obvious. By the seventh day, only the central area had fresh red spotted lesions, there was still a small amount of purpura, and edema and swelling have completely resolved; two weeks later, most of the water-retaining purpura becomes lighter changing from purple to dark red, reflecting the repair process after local microvascular rupture. The patient's right nasal region that received $CO_2$ laser therapy developed scar tissue. On the first day, the treatment region of the epidermis layer was lacking in the treatment area. If the leather tissue is exposed to pink, a small amount of oozing is crusted. On the third day, the entire treatment area was covered with dark red suede. On the fifth day, the skin thickened, and some areas appeared loose. On the seventh day, the edge of the edge area was off, and the pink neonatal tissue was basically consistent with the height of the skin, and the central area was still covered. After 14 days, the freshman tissue is reduced, skin color became close to normal, and a small amount of residual supper in the central area was about to fall off.

*4.3. Clinical Adverse Reactions.* The clinical adverse reaction example is four cases, and it is a scar formation of the upper lip area after 585 nm and 1064 nm double-wavelength laser. It has a series of laser treatments in patients with fresh red spots. Also, after multiple laser treatments to improve pigmentation, local pigment reduction has no significant improvement; there is a significant improvement in the treatment of $CO_2$ laser patients; for patients with thickened fresh red spots, after inappropriate doses of laser treatment, the skin shrinks in the lesion and develops into scar tissue.

## 5. Conclusions

The infrared thermal imagery is currently used in a wide range of noncontact modern temperature measuring instruments. It is widely used in the field. This paper uses light heat decomposition and photothermal solidification, laser plastic surgery, using the target base to absorb laser energy, physical and chemical changes and produces a series of biochemical reactions. Therefore, the dose in the treatment process is inaccurate, and the reasons for the increase in skin light sensitivity may result in excessive heat dissipation to the surrounding target group, causing adverse reactions and severe complications.

## Data Availability

The data used to support the findings of this study are available from the corresponding author upon request.

## Conflicts of Interest

The authors declare that there are no conflicts of interest.

## Authors' Contributions

Hong Wei and Fang Jiang contributed equally to this work.

## Acknowledgments

This study was funded by the study of the current situation and control countermeasures of occupational hazards of medical laser from the Hubei Province Key Laboratory of Occupational Hazard Identification and Control, Wuhan University of Science and Technology (No. OHIC2019G07), Wuhan 430065, China.

## References

[1] H. Yang, F. Xiong, K. Liu et al., "Research on temperature-assisted laser shock imprinting and forming stability," *Optics and Lasers in Engineering*, vol. 114, no. MAR, pp. 95–103, 2019.

[2] Q. Liu, C. Chengtao, Y. Huachun, and Z. Guocai, "Research and application of wireless temperature measurement device in high temperature enclosed environment," *International Polymer Processing*, vol. 31, no. 2, pp. 150–155, 2016.

[3] C. Yang, Y. Cai, C. Xin, and M. Shi, "Research on temperature error compensation method of vehicle-mounted laser gyro sins," *Journal of Physics: Conference Series*, vol. 1885, no. 4, p. 8, Article ID 042020, 2021.

[4] H. Zhao and J. Zheng, "Design and research on temperature control system of electric furnace based on plc touch screen integrated machine," *IOP Conference Series: Materials Science and Engineering*, vol. 914, no. 1, p. 6, Article ID 012034, 2020.

[5] R. P. Kale, A. Z. Kouzani, K. Walder, M. Berk, and S. J. Tye, "Evolution of optogenetic microdevices," *Neurophotonics*, vol. 2, no. 3, Article ID 031206, 2015.

[6] A. Tapetado, P. J. Pinzon, J. Zubia, and C. Vazquez, "Polymer optical fiber temperature sensor with dual-wavelength compensation of power fluctuations," *Journal of Lightwave Technology*, vol. 33, no. 13, p. 1, 2015.

[7] J. F. Brian, K. Wong, H. K. Kim et al., "The porcine and lagomorph septal cartilages: models for tissue engineering and morphologic cartilage research," *American Journal of Rhinology*, vol. 15, no. 2, pp. 109–116, 2018.

[8] E. Rainey and A. Kavner, "Peak scaling method to measure temperatures in the laser-heated diamond anvil cell and application to the thermal conductivity of mgo," *Journal of Geophysical Research Solid Earth*, vol. 119, no. 11, pp. 8154–8170, 2015.

[9] T. Zhou, C. Yao, Y. Hu, F. Yang, J. Wang, and M. Ouyang, "Research on performance and temperature control of glow plugs for ppci low load assist," *IFAC-PapersOnLine*, vol. 49, no. 11, pp. 223–230, 2016.

[10] E. Fanning, T. Donnelly, J. G. Lunney, D. B. Murray, and T. Persoons, "Application of gaseous laser-induced fluorescence in low-temperature convective heat transfer research," *Experiments in Fluids*, vol. 61, no. 5, pp. 1–20, 2020.

[11] F. Lin, J. Jin, J. Zheng, B. Shi, and T. Ren, "Review on application and research in temperature-adjusting asphalt pavements based on phase change materials," *Materials China*, vol. 36, no. 6, pp. 467–472, 2017.

[12] Y. Wang and C. Li, "Research on laser ablation technology in the material interaction of two-dimensional axisymmetric ablation model," *Journal of Physics: Conference Series*, vol. 1865, no. 2, p. 7, Article ID 022029, 2021.